Australian Heavy-Rain Days and Associated East Coast Cyclones: 1958–92

LINDA C. HOPKINS

Centre for Dynamical Meteorology, Monash University, Melbourne, Victoria, Australia

GREG J. HOLLAND

Bureau of Meteorology Research Centre, Melbourne, Victoria, Australia

(Manuscript received 9 December 1994, in final form 9 August 1996)

ABSTRACT

The authors present a comprehensive climatology of heavy rain and east coast cyclones from January 1958 to September 1992. A total of 80 cyclones, including nondeveloping systems, were objectively identified from daily rainfall and surface wind observations at 28 stations along the east coast of Australia. The method used first identifies heavy-rain days, then uses the wind observations to differentiate east coast cyclones from other rain-producing systems. This method is found to be reliable and with modifications may be used to identify other mesoscale systems.

In general, onshore southeasterly to southerly flow is most commonly associated with heavy rain along the east coast of Australia. Local convective heavy-rain events are most common in the Tropics, and the maximum occurrence of heavy-rain days propagates poleward from summer to winter. The latitudinal position and movement of the subtropical anticyclone, and variations in the Southern Oscillation index, have been found to be major factors in the variability of coastal heavy-rain occurrences.

Consistent with previous studies, it is found that east coast cyclones occur primarily in winter and form in regions of warm sea surface temperature anomalies. Intensification of east coast cyclones is associated with strong zonal sea surface temperature gradients, greater than 4°C within 50 km of the coastline.

Significant correlations exist between the occurrence of east coast cyclones, the Southern Oscillation index, and the latitudinal position of the subtropical anticyclone. The strongest correlations, however, suggest a preference for east coast cyclones to form between extreme episodes (negative to positive) of the Southern Oscillation index.

A long-term annual trend toward increased numbers of east coast cyclones has been identified, along with an apparent decrease of local convective heavy-rain events, particularly for coastal stations at higher latitudes. No corresponding trend is found for heavy-rain occurrences, the Southern Oscillation index, or the latitudinal position of the subtropical anticyclone.

1. Introduction

The geography of the Australian east coast is characterized by a western ocean boundary current, the East Australian Current (Fig. 1), and an extended coastal mountain range, known as the Great Divide (Fig. 2). The warm East Australian Current flows southward usually within 100 km of the continental shelf and terminates in the vicinity of Sydney (Harmon 1961). Poleward of Sydney, warm core anticyclonic oceanic eddies are shed from the East Australian Current and may be coastally trapped and/or drifting southward. Advection of warm tropical surface water around the developing eddies, combined with cold water moving equatorward near the shore produces strong coastal sea surface temperature gradients at higher latitudes. These gradients are especially strong in winter (Andrews 1979).

The coastal area east of the Great Divide experiences high rainfall variability and is vulnerable to heavy-rain producing systems such as tropical and midlatitude cyclones (Sinclair 1994). Previous rainfall studies have shown that annual and seasonal rainfall is strongly correlated to the El Niño–Southern Oscillation (ENSO). Drier than normal conditions over Australia, occur when the Southern Oscillation index (SOI) is strongly negative—that is, El Niño episodes (Ropelewski and Halpert 1987; Whetton et al. 1990; Allan et al. 1990)—while wetter than average conditions in eastern Australia have been shown by Ropelewski and Halpert (1987, 1989) and Kiladis and Diaz (1989), to be associated with La Niña or high SOI events. Above average Australian regional rainfall and a high SOI have also been associated with anomalous warm sea surface temperatures (SST) (Streten 1983; Lough 1992; Cordery and Opoku-Ankomah 1994), and a poleward shift of the subtropical

Corresponding author address: Linda C. Hopkins, Bureau of Meteorology Research Centre, GPO Box 1289K, Melbourne, Victoria 3001, Australia.

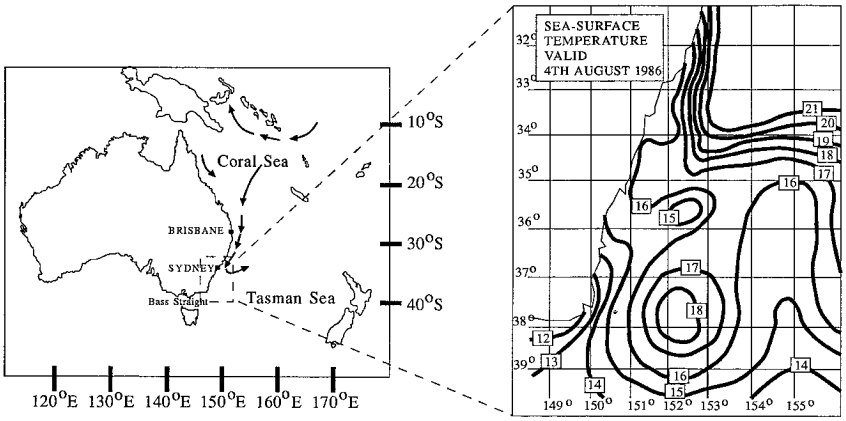

FIG. 1. Map of Australia and relevant geographical locations. Arrows indicate the general direction of oceanic currents affecting the east coast of Australia. Inset: ''Snapshot'' of the East Australian Current below 31°S, valid the week beginning 4 August 1986, shows the southern extremity of the East Australian Current and the presence of warm and cold core eddies. SST in degrees Celcius.

anticyclone (STAC) (Pittock 1973; Lough 1991). However, Yu and Neil (1991), have shown that high intensity rainfall ($>$40 mm day^{-1}) may not necessarily follow the same pattern as average rainfall. Nicholls and Kariko (1993) demonstrated that Australian rainfall is correlated to the SOI, not only by simple increases and decreases in annually averaged rainfall, but by increases/decreases in the intensity of the rainfall, and related continuous rain days. It is then of no surprise that the El Niño–SOI has been strongly related to tropical cyclone activity in Australia (Nicholls 1984; Hastings 1990), suggesting that not only average rainfall but heavy-rain producing systems may be related to the SOI and the STAC.

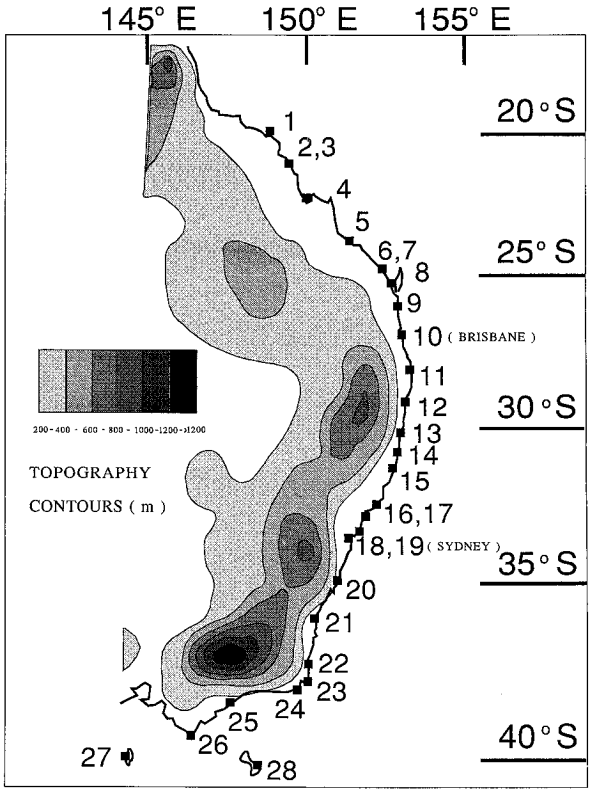

FIG. 2. Geographical locations of the 28 stations employed in this climatology and their relative positions to topography at 200-m contour intervals. Stations 2 and 3 and 6 and 7 are represented as one square due to their close proximity to each other.

One coastal heavy-rain producing system is the Australian east coast cyclone (ECC). These low pressure systems differ from other coastal lows in that their subsequent movement follows the eastern coastline. Flood climatologies by Colls (1991, personal communication) and Speer and Geerts (1994) have demonstrated that east coast cyclones are a primary cause of flooding in the Sydney Metropolitan area, while individual case studies of east coast cyclones (Holland et al. 1987; Leslie et al. 1987; Lynch 1987; McInnes and Hess 1992; McInnes et al. 1992) show average daily rainfall totals in excess of 50 mm day^{-1} and observed spot peak values of 200–300 mm day^{-1}. The size of east coast cyclones range from 50 to 1000 km (Holland et al. 1987), with the more synoptic-scale systems often referred to as east coast lows or coastal cutoff lows (McInnes and Hess 1992; McInnes et al. 1992). Australian east coast cyclones, although variable in size and intensity, are typically characterized by widespread heavy rainfall.

The reason for such associated heavy rain may be found from the large-scale synoptic environment in which they form. Figure 3 shows mean sea level pressure (MSLP), 300-hPa geopotential height, and winds for an east coast cyclone that occurred in August 1990. Formation typically occurs when an upper-level shortwave trough or cutoff low moves over an area of strong low-level baroclinicity (Holland et al. 1987; McInnes et al. 1992). Callaghan (1986) showed that during coast-

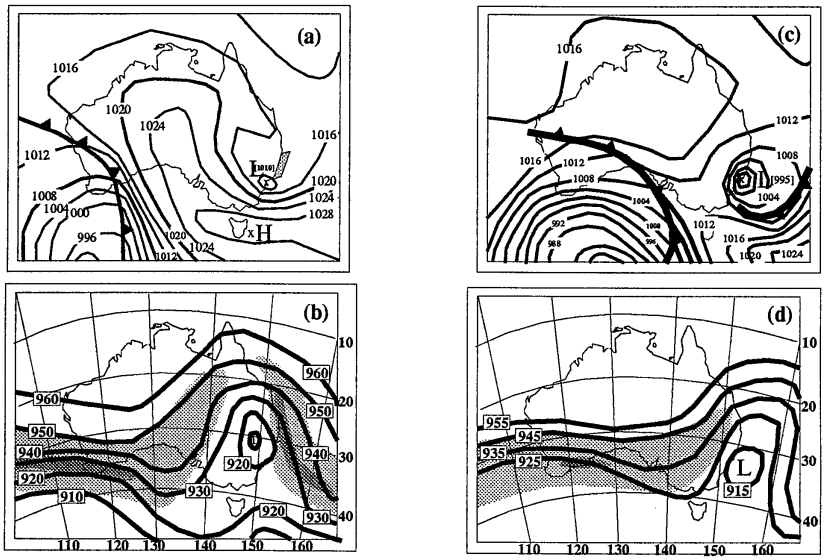

FIG. 3. National Meteorological Centre of the Australian Bureau of Meteorology MSLP analyses (4-hPa intervals) for 0000 UTC on (a) 2 August 1990 [shaded area indicates an east (warm)–west (cool) SST gradient of 7°C], and (c) 3 August 1990. Corresponding 300-hPa geopotential height (10-dm intervals) for 0000 UTC on (b) 2 August 1990 and (d) 3 August 1990. Light shading indicates 100–150 kt winds and dark shading, winds over 150 kt.

al cyclogenesis, a mobile 500-hPa westerly cutoff low is found moving eastward, toward the coast prior to cyclogenesis. This is consistent with the Holland et al. (1987) findings of a poleward dip in the surface easterlies, equatorward of a blocking high (easterly dip), as a precursor to cyclogenesis. The coastal mountain range not only provides orographic uplift, but is a mechanism for cyclonic northward deflection of the low-level easterly flow, resulting in cyclogenesis and convection (Leslie et al. 1987). In winter, this effect is enhanced in the presence of anomalously warm coastal waters, resulting in a strong local zonal SST gradient (Fig. 3a). Warm moist tropical air is adiabatically lifted, while being advected around the poleward side of the easterly dip or cyclone, as it moves over increasingly cooler surface temperatures.

Though not as widely documented or as common as tropical cyclones, Australian east coast cyclones affect large populated cities such as Sydney and Brisbane (Fig. 1), between which over one-third of the population of Australia resides. They are considered a major forecasting problem due to their capacity for rapid intensification (Holland et al. 1987; Lynch 1987), satisfying the ''Bomb'' criterion of Sanders and Gyakum (1980). Not all east coast cyclones undergo rapid intensification and strong winds, however. All, however, produce widespread heavy rain, due to ascent of warm equatorial air moving around the poleward side of the low, and high onshore winds arising from an increase in pressure gradients between the poleward moving low pressure system and a blocking high (Fig. 3). Rain associated damages attributed to east coast cyclones are estimated in millions to tens of million dollars annually and are a major contributor to the total weather-associated insurance losses for all of Australia.

In this paper, we utilize heavy-rain days, as defined in section 2, together with wind observations for a string of stations along the east coast of Australia, to derive an objective climatology of Australian east coast cyclones from 1958 to 1992. Our aims are to identify the preferred season, location, and long-term trends of heavy coastal rainfall and associated east coast cyclones. The relationships between the Southern Oscillation Index, the subtropical anticyclone, east coast cyclones, and heavy-rain days are also investigated.

A previous climatology (Holland et al. 1987) was not sufficiently consistent nor long enough to develop detailed statistics of occurrence and effect, including long-term trends. A climatology based solely on published daily MSLP charts from the National Meteorological Centre of the Australian Bureau of Meteorology (NMC), was considered unreliable, owing to the relatively small size and duration of these systems, changing analysis trends, and difficulties with analyzing systems over the ocean area before the satellite era. Our initial analysis indicated that although many systems may be difficult to locate on charts, the associated rainfall is commonly widespread and extensive. We therefore chose to use a 34-yr record of daily rainfall and surface wind data from a roughly even distribution of 28 stations lying between 20° and 40° S along the east coast of Australia (Fig. 2). Since these stations have not changed significantly during this period, quantitative patterns of trends and effects of east coast cyclones can be developed.

Section 2 of this paper deals with the methodology of classifying heavy-rain and wind events into a co-

herent order for identification of east coast cyclones. The resulting climatology of east coast cyclones and heavy rainfall is investigated in section 3, and our major conclusions are presented in section 4.

2. Methodology

a. Definition of an east coast cyclone

A number of local studies have examined east coast cyclones, but few have been published and there is some confusion regarding what constitutes an east coast cyclone. The definition employed in this paper is a slightly modified version of the working definition used by the New South Wales Regional Office of the Bureau of Meteorology:

Any system with closed cyclonic circulation at sea level, which forms in a maritime environment between 20° and 40°S and within 500 km of the eastern coastline of Australia. The low pressure system must exhibit at some stage of its lifetime a component of movement parallel to the coastline and have a pressure gradient of at least 4 hPa (100 km)$^{-1}$.

We note that while east coast cyclones are not tropical cyclones, we include in the above definition any tropical cyclone moving into higher latitudes.

b. Database

Following a careful examination, the 28 stations in the appendix and Fig. 2 were selected for analysis. These stations reported consistently throughout the period and provide a roughly even distribution of observations along the east coast of Australia between 20° and 40°S. A database of surface wind and daily rainfall from January 1958 to September 1992 was compiled for each station. Three stations were not operational in 1958. One of these was replaced by a nearby station (station 2 to 3) with no data loss and the remaining two were deemed to be sufficiently covered by the surrounding stations. One possible systematic bias in the rainfall records arises from the change from imperial (British) to metric units at the start of 1974. Lavery et al. (1992) and Nicholls and Kariko (1993) found no obvious bias in the Australian rainfall records from this change of units.

The daily rainfall dataset is quite comprehensive, with all but five stations having an unbroken record for the analysis period. Station 1, Hayman Island, was the most unreliable and contained lengthy gaps in its record, but because of its location on the northern extremity of the dataset, was considered acceptable for our purposes. Data collected from station 6 although having an unbroken record was considered poor due to known positional problems with the rain gauge and hence was used only to supplement station 7, which had lengthy gaps (in the order of years). The overlap between stations 6 and 7 was in good agreement, except in summer, resulting in a possible overestimation of heavy-rain days for this period. The remaining three stations were missing only occasional months of data.

The surface wind data are not so comprehensive, and were collected at odd times and at different intervals. For example, at some stations 3-h surface-wind observations were taken, but the observing times differ; at other stations surface-wind data were only collected every 12 h. Because of this variability of observing times and inconsistent anemometer heights, our climatology is initially developed from the rainfall data, then refined using the wind data.

Supporting analyses were obtained from the routinely published NMC MSLP charts, NMC Australian monthly climatological SST, and weekly SST charts for the western Tasman Sea, compiled by the Royal Australian Navy for the 7-yr period 1982–88. Monthly SOI data were provided by the National Climate Centre of the Australian Bureau of Meteorology, for the period 1958–92. The SOI data used, is defined as the standard (mean = 0; standard deviation = 10) difference in MSLP between Darwin (Australia) and Papeete (Tahiti). Ten-year averaged, global (3° × 3° resolution), 1200 UTC analysis charts from European Centre for Medium-Range Weather Forecasts were obtained as a monthly climatological dataset. Mean monthly latitudinal positions of the subtropical surface high pressure belt, or subtropical anticyclone, were obtained from Pittock (1973) and updated to 1981 (Pittock, 1994 personal communication).

c. Method

We expect that the rainfall associated with an east coast cyclone will be heavy and occur over a number of stations within a minimum time period. However, heavy rain is a very subjective concept, as indicated by the monthly mean rainfall in Figs. 4a–d. The four panels are roughly indicative of coastal stations between latitudes: (a) 20°–25°, (b) 25.5°–31°, (c) 31.5°–36°, and (d) 37°–40°S. The oscillation between wet summers and dry winters is apparent for subtropical stations north of 37.5°S (stations 1–23). The tropical influence decreases in amplitude with higher latitudes. Stations 24–28 on the Australian south coast are influenced by maritime systems originating from waters south of the continent and experience a midlatitude climate of wet winter months and dry summer months. To remove such seasonality and local effects, we define a heavy-rain day for an individual station as one in which the daily rainfall exceeds 10 times its long-term monthly mean daily rainfall. We next define a heavy-rain event as a set of heavy-rain days that are related temporally and spatially. The method used to identify heavy-rain events is illustrated in Fig. 5. Thus,

1) all heavy-rain days that occur on the same or sequential days are collated together, regardless of station location;
2) all heavy-rain days that occur at stations within 300

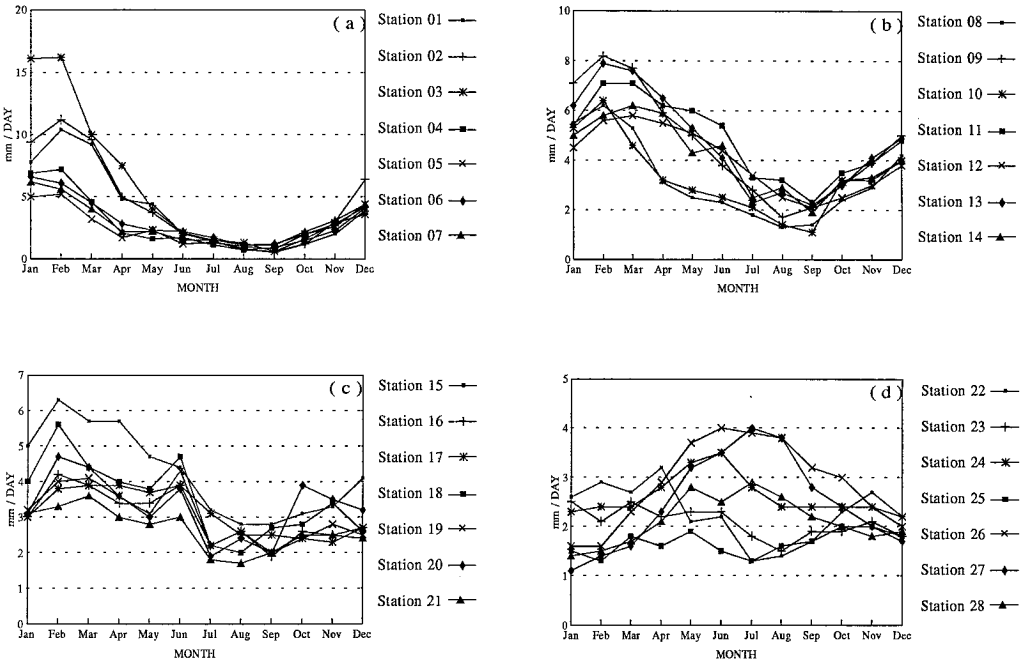

FIG. 4. Long-term monthly mean daily rainfall for (a) stations 1–7 (20°–25°S); (b) stations 8–14 (25.5°–31°S); (c) stations 15–21 (31.5°–36°S); (d) stations 22–28 (37°–40°S).

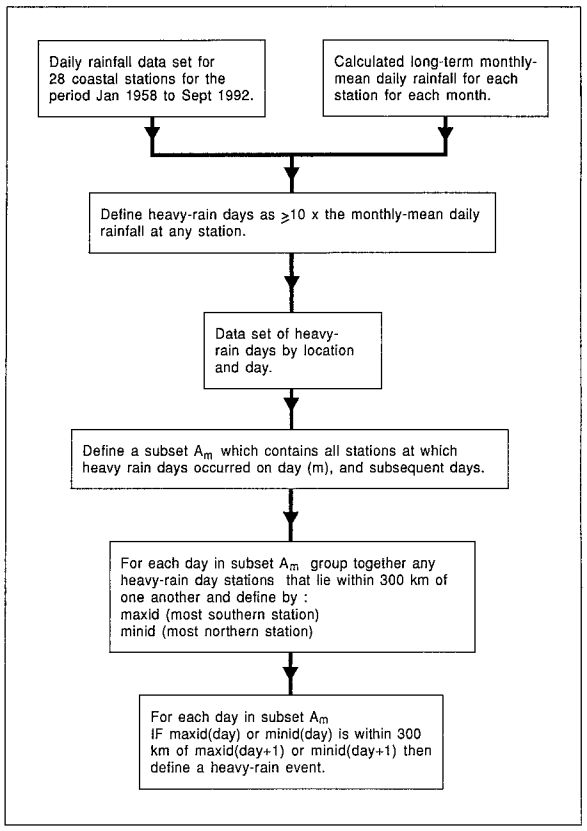

FIG. 5. Flow chart depicting the method used to define a heavy-rain event.

km are defined as compromising a heavy-rain event. A 300-km separation distance is purely arbitrary, and based on the assumption that if a heavy-rain day occurs at two stations more than 300 km apart and at no stations in between, it is the result of two different weather systems.

In this way a heavy-rain event is characterized by the number of days over which the event occurred, its location within the study domain, and the size, defined by the spread of stations that experience heavy rain. It must be remembered, however, that the term heavy-rain day refers to a particular station having heavy rain on one particular day. This means that we can in fact have a maximum of 28 heavy-rain days occurring on any one day. To avoid any confusion when using the term ''day'' in an annual, seasonal, or monthly total for all 28 stations, we use the term ''heavy-rain occurrence'' to describe the number of heavy-rain days occurring over a number of stations over a set period of time. Heavy rain isolated to one station on any day is considered to arise from local convection and is defined as a local convective heavy-rain event.

We disregard local convective-rain events and all events lasting less than one day when defining an east coast cyclone. The rationale derives from our working definition and an expectation that the synoptic situation will maintain the associated coastal rainfall for a significant time. In this way, we may appear to be explicitly excluding the small type 1 and 3 systems described by Holland et al. (1987), which are short lived and mainly

associated with localized strong winds. However, these are normally associated with a larger, longer-lived low pressure system and onshore flow, which produce heavy rain, and the type 1 and 3 subsystems are identified by surface wind data. Tropical cyclones are removed from the database by excluding events confined to stations north of 25°S during the cyclone season of November–March. Decayed tropical cyclones moving down the east coast were included, provided that they satisfied our working definition. Rainfall associated with midlatitude systems passing through Bass Strait (Fig. 1), was excluded by requiring that at least one station in any event must have been equatorward of station 24 (Fig. 2).

We compared heavy-rain events derived from this process with east coast cyclones from the period 1980–92 identified from previous studies and from the MSLP analyses archived at NMC. Factors such as size and duration of heavy-rain events, size-to-duration ratio, and mean and maximum rainfall, provided no clear relationships. This is not surprising, since frontal systems and easterly troughs are also associated with heavy rainfall, as noted in Speer and Geerts (1994). Surface wind data were therefore used to identify the east coast cyclones amongst the heavy-rain events.

Three hourly time series of surface winds, starting at 0000 UTC on day 1 of the event, were constructed for all stations included in each heavy-rain event lasting more than one day. Data collected at times not corresponding to the 3-h intervals, were simply translated to the nearest defined hour. Maritime cyclones close to the coastline were then objectively identified by the following signature: that coastal stations show a consistent southerly wind component for the same time period; and the winds turn with time, clockwise for systems moving down the coast and anticlockwise for equatorward motion. Systems that originate inland are identified from a northerly to southerly change in surface winds as they move out to sea, and are excluded from the dataset.

Daily MSLP charts from the NMC and previous studies were used to check our method for the period 1980–92. All known east coast cyclones were detected by the combined rain and wind method. Previously unidentified systems were validated from a reexamination of all analysis data. Thus, the method seems capable of objectively identifying all east coast cyclones that satisfy our working definition.

The 23 identified east coast cyclones that occurred in the 1982–88 period of available weekly SST analyses were then placed into eight categories for analysis (Table 3). We started with the three types of east coast cyclone defined by Holland et al. (1987) and added a transitioning tropical cyclone as type 4. Using daily NMC charts, systems were classified into developers (D) if they intensified at greater than 4 hPa d^{-1} within 500 km of the coast after formation. The remainder were classified as nondevelopers (ND). Types 1 and 3 were identified by their being embedded in the heavy rain producing synoptic flow.

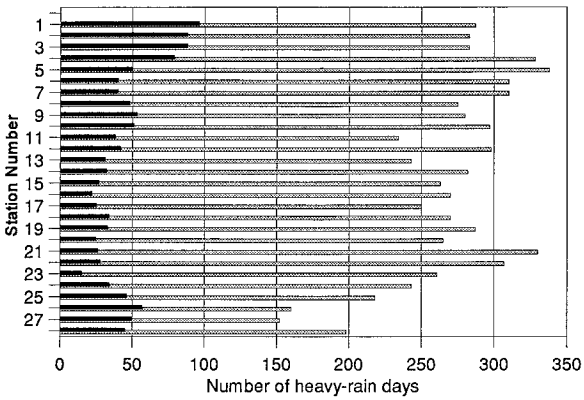

FIG. 6. Number of local convective heavy-rain events (solid black bar) and heavy-rain days (gray bar), for each station between January 1958–September 1992. A composite has been used for stations 2,3 and 6,7.

Linear and partial correlations are used to demonstrate relationships between east coast cyclones, heavy-rain occurrences and climatic parameters such as the Southern Oscillation Index and the latitudinal position of the subtropical anticyclone. Correlations are calculated as in standard textbooks and confidence levels are determined using a Student's two tailed t-test (Moore and McCabe 1993). Following standard practice, correlations using annual averages are taken from April through to the following March, to capture the annual SOI signal and El Niño and La Niña episodes.

3. Results

a. Heavy-rain days

The histogram for all heavy-rain days and local convective heavy-rain events at a particular station (Fig. 6) displays some spatial variability. This is possibly associated with topographic enhancement and local effects. In total, 6833 heavy-rain days are identified for all 28 stations over the period 1958–92, with 16.5% associated with local convective heavy-rain events. The spatial distribution of heavy-rain days is relatively uniform north of station 25 (Fig. 2), with fewer heavy-rain days identified south of here. Overall, the distribution is consistent enough to group all heavy-rain days together to gain an insight into the temporal distribution of heavy-rain occurrences affecting the coastal region of eastern Australia between 20° and 40°S.

From station 1, a steady poleward decrease in the number of local convective heavy-rain events is evident to station 24. This is consistent with decreasing incidence of localized convective storms away from the Tropics. The trend is reversed at higher latitudes as a result of the passage of midlatitude systems moving rapidly through Bass Strait (Figs. 1 and 2). On a seasonal

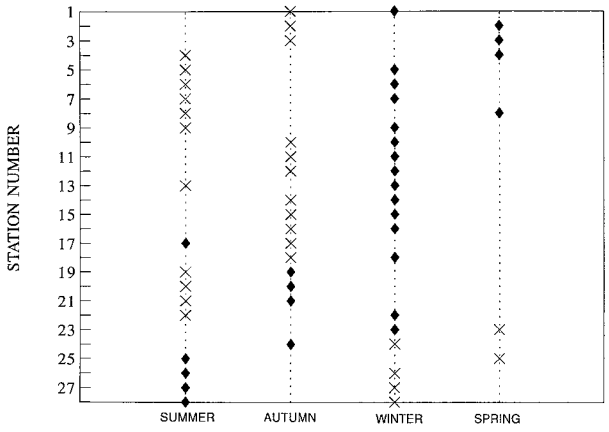

FIG. 7. Plot showing the most frequent ♦ and least frequent × heavy-rain days with season.

basis, Fig. 7 demonstrates a coherent pattern of maximum number of heavy-rain days with latitude. The maximum frequency (diamonds) of heavy-rain days occurs at high latitudes during summer and moves consistently to tropical stations in winter. These findings suggest that the seasonal movement of heavy rain may be related to the seasonal movement of the subtropical anticyclone (Fig. 8) from its most poleward position in winter to most equatorward in summer. In contrast to heavy-rain days, local convective heavy-rain events (not shown), show no consistent latitudinal movement with season.

Table 1 shows linear, partial, and lag correlations of heavy-rain occurrences (HRO), east coast cyclones (ECC), and the SOI, with the latitudinal position of the subtropical anticyclone (STAC), for the period 1958–81. A poleward shift of the STAC appears to be significantly related to increased heavy-rain occurrences at all timescales, with the possible exception of the winter months. The STAC itself shows poor correlation with the SOI except in the summer months, where a poleward (equatorward) shift in the latitudinal position occurs with positive (negative) SOI values. Partial correlations show that this summer relationship reflects correlations, of both variables with heavy-rain occurrences. When relationships with heavy-rain occurrences are removed, a strong, in-phase correlation between the SOI and STAC is revealed in winter. Monthly correlations with the SOI are poor due to the noisiness of the SOI signal at small timescales. Lag correlations reveal an increased (decreased) frequency of heavy-rain days in spring after a poleward (equatorward) shift of the STAC from its mean position in the previous three seasons.

Linear and partial correlations of heavy-rain occurrences with the SOI (Tables 1 and 2) show significant, in-phase relationships, especially in summer and winter. Increased frequency of heavy-rain occurrences in summer appears to be associated with a positive SOI in the previous winter/spring.

Figure 9 shows the 24-h mean wind direction for heavy-rain occurrences and local convective heavy-rain

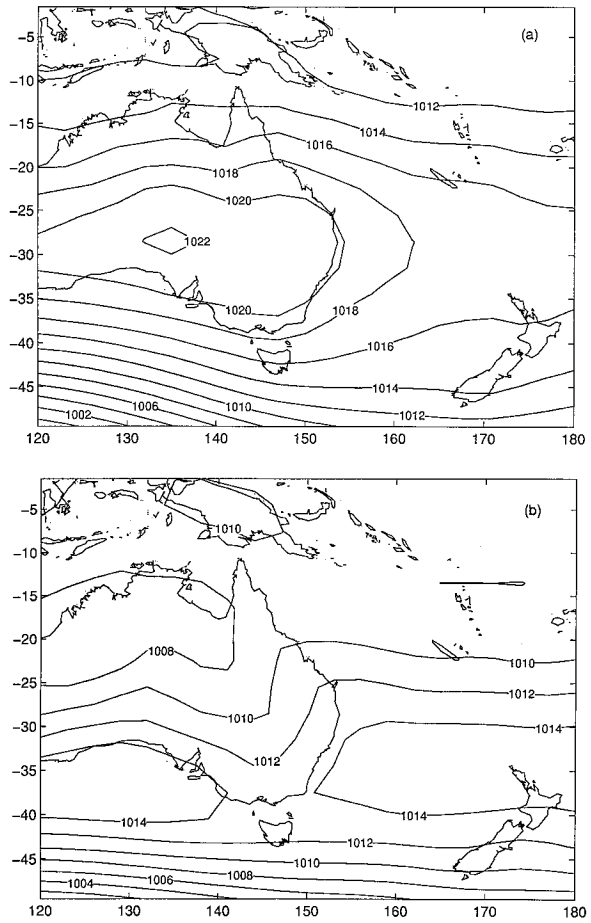

FIG. 8. ECMWF 10-yr climatological MSLP for (a) winter and (b) summer, showing the two extreme positions of the subtropical anticyclone.

events. Southerly to southeasterly flow dominates, consistent with onshore flow and orographic uplift. A more detailed breakdown for all stations (Fig. 10) indicates that most frequent heavy-rain events (convective or otherwise) occur under a consistent flow at an angle of around 20°–30° to the left of a unit vector **n** pointed equatorward and parallel to the coastline. This is consistent with convergence and uplift of cyclonic onshore easterly flow by the coastal mountain range.

b. East coast cyclones

Eighty east coast cyclones were identified between January 1958 and September 1992, with their associated heavy rain accounting for about 16% of all heavy-rain occurrences. The mean monthly distribution (Fig. 11) shows a preference for formation in the autumn/winter months, agreeing with previous studies (Holland et al. 1987; Sinclair 1994). Australian autumn/winter is when the land–sea temperature difference is becoming greatest, and the subtropical anticyclone shifts equatorward (Fig. 8).

TABLE 1. Correlations between the STAC and the SOI, HRO, and ECC, between 1958 and 1981. Here, n denotes the population sample. The linear, partial, and lag correlation coefficients (r), are indicated for each of the four seasons, seasonal, monthly, and the annual average. Confidence levels of 95% (*) and 99% (**) are shown. Only lag correlations above the 95% confidence level are shown.

	Annual n = 23	Seasonal n = 95	Monthly n = 288	Summer n = 23	Autumn n = 24	Winter n = 24	Spring n = 24
$r_{stac,hro}$	−0.58**	−0.392**	−0.355**	−0.687**	−0.573**	−0.272*	−0.726**
$r_{stac,soi}$	−0.262*	−0.065	−0.01	−0.542**	−0.183	0.213	−0.043
$r_{hro,soi}$	0.552**	0.393**	0.316**	0.623**	0.235	0.414**	0.262
$r_{stac,ecc}$	−0.3*	−0.092	−0.189**	−0.423**	−0.46**	−0.192	−0.183
$r_{ecc,soi}$	0.275*	0.161**	0.171**	0.256	0.158	0.085	0.202
$r_{ecc,hro}$	0.613**	0.525**	0.475**	0.67**	0.514**	0.714**	0.377**
Partial correlations							
$r_{(stac\ hro),soi}$	−0.536**	−0.4**	−0.371**	−0.53**	−0.555**	−0.405**	−0.741**
$r_{(stachro),ecc}$	−0.526**	−0.406**	−0.307**	−0.6**	−0.442**	−0.196	−0.722**
$r_{(stac\ soi),hro}$	0.027	0.11	0.115*	−0.2	−0.061	0.372**	0.222
$r_{(stac\ soi),ecc}$	−0.196	−0.051	−0.023	−0.495**	−0.126	0.235	−0.006
$r_{(soi\ hro),stac}$	0.425**	0.4**	0.334**	0.41**	0.162	0.502**	0.336**
$r_{(soi\ hro),ecc}$	0.505**	0.367**	0.271**	0.63**	0.182	0.507**	0.205
$r_{(stac\ ecc),soi}$	−0.246	−0.083	−0.19**	−0.35**	−0.444**	−0.216	−0.178
$r_{(stac\ ecc),hro}$	−0.086	0.145*	−0.025	0.07	−0.235	0.003	0.142
$r_{(ecc\ hro),stac}$	0.565**	0.534**	0.444**	0.576**	0.344**	0.701**	0.361**
$r_{(hro\ ecc),soi}$	0.575**	0.509**	0.45**	0.675**	0.497**	0.748**	0.343**
$r_{(soi\ ecc),hro}$	−0.097	−0.058	0.025	−0.28*	0.045	−0.33**	0.116
$r_{(soi\ ecc),stac}$	0.213	0.156*	0.172**	0.035	0.085	0.131	0.198

Significant lag correlations

	Autumn STAC next spring HRO	Winter STAC next spring HRO	Summer STAC next spring HRO	Summer STAC next spring ECC
r	−0.39**	−0.395**	−0.309*	0.368**

TABLE 2. Correlations between the SOI, HRO, and ECC, between 1958 and 1992. Here, n denotes the population sample. The linear, partial, and lag correlation coefficients (r), are indicated for each of the four seasons, seasonal, and the annual average. Confidence levels of 95% (*) and 99% (**) are shown. Only lag correlations above the 95% confidence level are shown. Coherence values for the yearly averaged time series of ECC and the SOI, in addition to correlations of HRO and ECC with the interannual differences of the SOI, defined as $SOI_{(yr+1)} - SOI_{(yr-1)}$ or $SOI_{(yr+1)} - SOI_{yr}$, are presented.

HRO-SOI; ECC-SOI; ECC-HRO (1958–1991)

	Annual n = 33	Seasonal n = 135	Summer n = 33	Autumn n = 34	Winter n = 34	Spring n = 34
$r_{soi,hro}$	0.558**	0.363**	0.601**	0.238*	0.371**	0.23
$r_{soi,ecc}$	0.23*	0.115*	0.176	0.026*	0.104	0.2
$r_{ecc,hro}$	0.537**	0.482**	0.532**	0.623**	0.539**	0.309**
Partial correlations						
$r_{(soi\ hro),ecc}$	0.53**	0.353**	0.609**	0.284**	0.376**	0.181
$r_{(soi\ ecc),hro}$	−0.1	−0.073	−0.212	−0.161	−0.123	0.14
$r_{(ecc\ hro),soi}$	0.506**	0.476**	0.542**	0.635**	0.542**	0.276**

Significant lag correlations

	Winter SOI next summer HRO	Spring SOI next summer HRO	Spring SOI next summer ECC	Summer SOI next ECC
r	0.343**	0.569**	0.329**	−0.575**

Coherence of ECC and SOI

Maximum coherence	Period (yrs)	Transfer function phase
0.882**	4.5	81.1°

Interannual differences of the SOI correlations

	$SOI_{(yr+1)-yr}$, HRO_{yr+1}	$SOI_{(yr+1)-(yr-1)}$, HRO_{yr}	$SOI_{(yr+1)-yr}$, ECC_{yr+1}	$SOI_{(yr+1)-(yr-1)}$, ECC_{yr}
r	0.490**	0.103	0.399**	0.485**

TABLE 3. Summary of results from a 7-yr climatology of nondeveloping (ND) and developing (D) east coast cyclones for the period 1982–88.

Definition	Forms within a land-centered easterly dip		Forms within an off-shore easterly dip		Forms with a large low in the Tasman Sea		Transitioning tropical cyclone	
Region of formation	<25°S		20°–40°S		<30°S		>25°S	
Direction of movement along the coast	N → S		N → S		S → N		N → S	
Duration of time spent on the coast	<1 Day		>1 Day		<1 Day		>1 Day	
	ND	D	ND	D	ND	D	ND	D
Number	1	3	6	7	1	3	1	1
Preferred season of formation	*	*	Aut	Win	*	*	*	*
SST gradient within ½° of coast	2°	>4°	<3°	>4°	4°	>4°	N/A	5°
Ave. SST anomaly near region of formation °C	5.5°	1.5°	2.3°	2.7°	2°	2.6°	N/A	1°
Ave. associated heavy rainfall (mm/day^{-1})	67.5	55.4	64.3	54.6	45.3	24.1	142	68
Ave. associated surface winds (m s^{-1})	7.7	17.3	14	17.5	14.4	23.2	11.3	23

* Denotes insufficient data to determine a clear preferred season of formation. N/A denotes data unavailable.

Linear, partial, and lag correlations of Australian east coast cyclones (ECC), with the STAC are shown in Table 1. Strongest linear correlations occur annually and in the summer and autumn seasons, when a poleward shift of the latitudinal position of the STAC from the mean usually coincides with an increase in east coast cyclones. However, partial correlations show that this reflects the strong correlations of heavy-rain occurrences with the SOI and ECC. The strong correlation between ECC and HRO, Tables 1 and 2, is compatible with our method of defining an east coast cyclone. Weak in-phase, annual, and seasonal correlations of ECC with the SOI, Tables 1 and 2, are primarily due to a lack of linear correlation in the autumn/winter months. After the effects of HRO are removed, partial correlations reveal that large negative values of the SOI are related to increased numbers of ECC in summer and winter. Lag correlations show a positive relationship between spring SOI value, and ECC the following summer. This correlation is consistent with Nicholls (1985, 1992), and may be related to transitioning tropical cyclones. The most significant lag correlation (−0.575), however, oc-

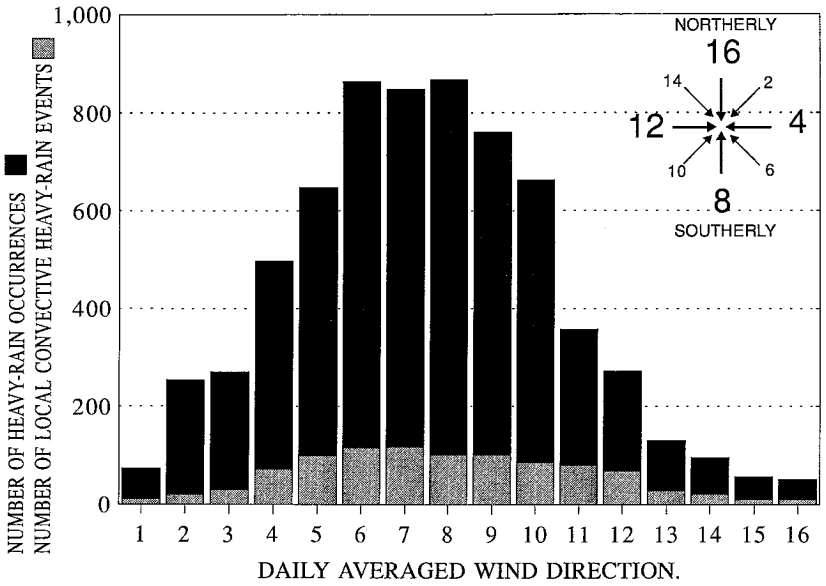

FIG. 9. Histogram, using all 28 stations, indicating the daily averaged wind direction for local convective heavy-rain events (light gray bars), superimposed upon the number of heavy-rain occurrences (black bars), for the period January 1958–September 1992.

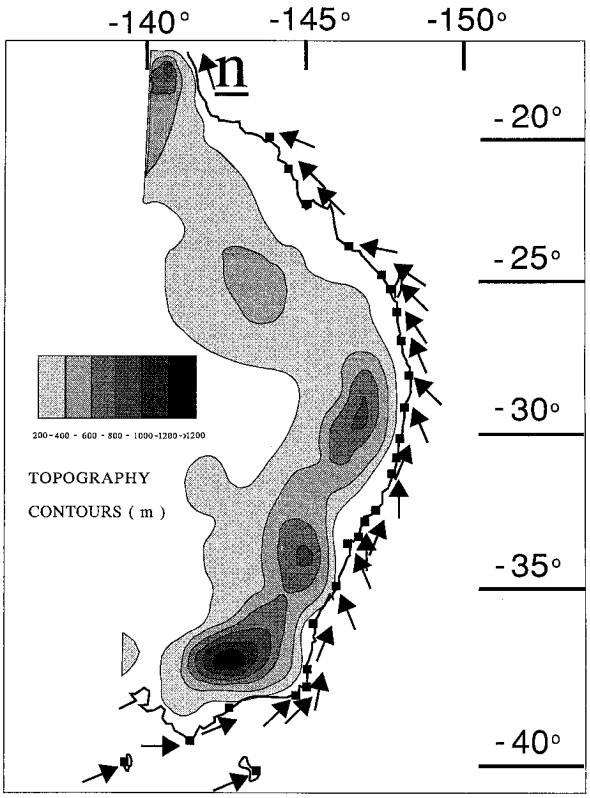

FIG. 10. Most frequent daily averaged wind direction (arrows), of heavy-rain occurrences, for all 28 stations used in this study. Station location and topography are as in Fig. 2. The vector ***n*** lies parallel to the coastline, pointing in a northward sense.

curs between SOI values in summer and numbers of east coast cyclones in the following spring.

The overall low correlation between SOI and ECC is surprising, given the strong correlations between SOI-HRO and HRO-ECC. A Fourier decomposition of the SOI and ECC time series (Table 2) indicates that the two time series are almost 90° out of phase with each other, with a strong coherence in the 4.5-yr, El Niño–Southern Oscillation timescale. This suggests that the frequency of ECC may be related not to the raw SOI point data, but the interannual differences of the SOI defined as the difference between annual SOI value at one year and the next year, or one year and two years later. Correlations of ECC with the interannual differences of the SOI (Table 2) indicate a strong preference for ECC to form just after a large swing from negative to positive SOI values and especially between swings from negative SOI the year before and positive SOI the year after. This suggests a preference for formation of east coast cyclones between extreme events of the Southern Oscillation index, as demonstrated in Fig. 12.

The characteristics of eight categories of east coast cyclones (section 2) occurring during the 7-yr period of available SST records are summarized in Table 3. Type 2 east coast cyclones are the most common and long lived, with movement and associated widespread rainfall being dominated by the larger synoptic pattern. They form anywhere within the domain and have a preference for intensification in the winter months. Types 1 and 3 tend to be explosive short-lived systems (Holland et al. 1987), and appear to be restricted to the midlatitudes. They are commonly associated with preexisting lows

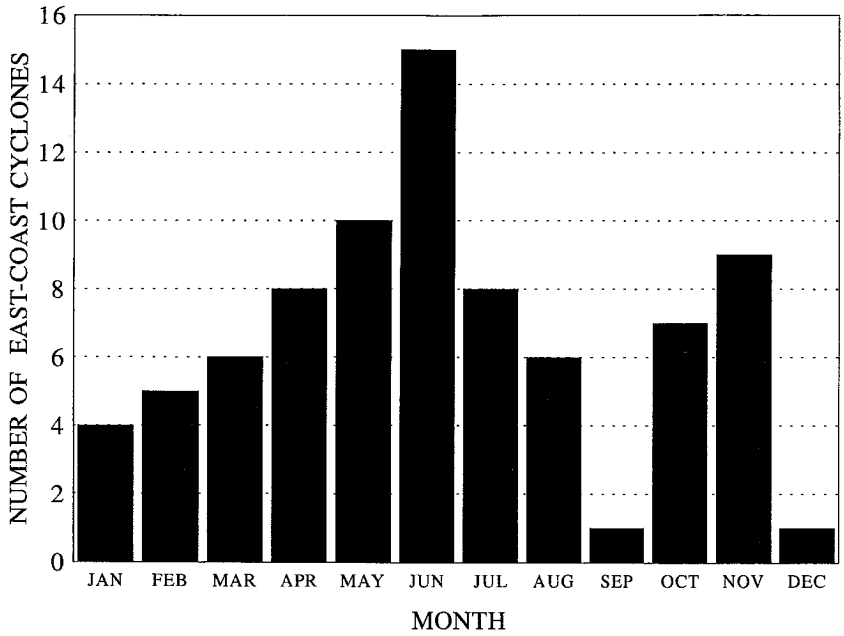

FIG. 11. Histogram of east coast cyclones (January 1958–September 1992), showing a preference for formation in cooler months.

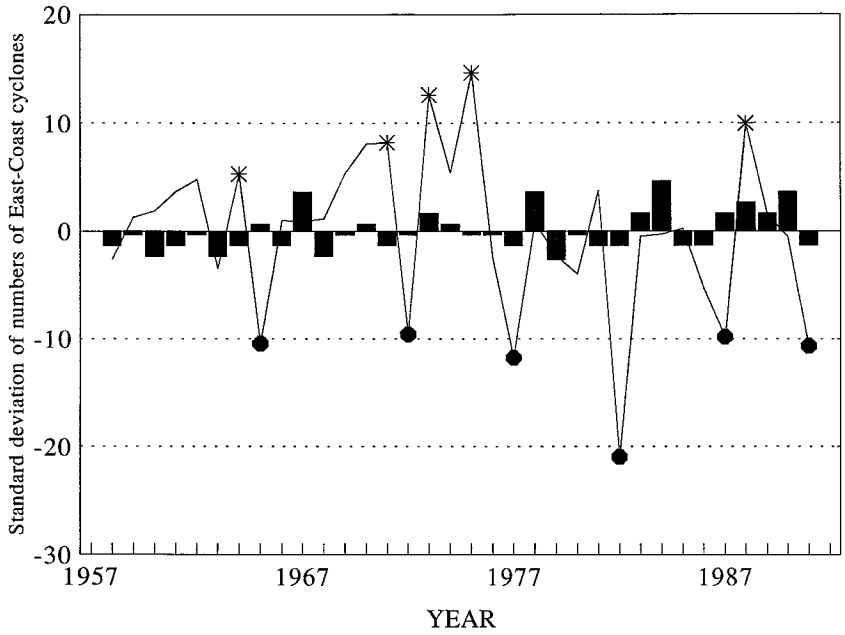

FIG. 12. Annual deviation of east coast cyclone occurrence from the long-term mean (bar graph) and the annual SOI time series. Documented El Niño (o) and La Niña (*) events are indicated.

and hence their movement along the coastline is intimately influenced by the relative locations of these low pressure systems. For example, type 3 cyclones cyclonically orbit an associated low out in the Tasman Sea and move equatorward.

Nowra Naval Weather Centre weekly SST analyses and monthly climatological SST charts from NMC confirm that all of the identified systems form in the presence of substantial warm SST anomalies. The near coastal oceanic region below 34°S is an extremely dynamic environment, with warm and cold core oceanic eddies of the type shown in Fig. 1 moving and merging at timescales in the order of a week. Hence, SST anomalies were derived near where the surface cyclone formed and only SST gradients associated with the path of the surface cyclone were used. There is no direct relationship between the magnitude of the SST anomaly and intensification of the cyclone. Rather, intensification is associated with strong SST gradients close to the coastline, which is consistent with numerical studies (e.g., Leslie et al. 1987; McInnes et al. 1992).

Surprisingly, for all types the average coastal rainfall associated with nondeveloping cyclones is heavier than that for developing systems. This was confirmed by checking available rain analyses. Such a finding may be due to the tendency for heavy, but short-lived rainfall over a restricted area that accompanies intense east coast cyclones, compared to the characteristically longer-lived widespread rainfall for nondeveloping systems. Surface winds were stronger for developers, as expected.

c. Long-term trends: 1958–91

Heavy-rain occurrences and isolated convective heavy-rain events for stations have been grouped into 5° latitude belts, with the exception of those south of station 19 where a grouping from 35° to 37.5°S and 37.5°–40°S is defined to delineate any midlatitude systems moving across Bass Strait (Figs. 2 and 6). A summary of linear trends between 1958 and 1991 is shown in Fig. 13 and Table 4. There is no significant trend with time for heavy-rain occurrences (Fig. 13a). But a marked overall decline has occurred in local convective heavy-rain events, which is highest at higher latitudes (Fig. 13b).

A trend toward increasing frequency of Australian east coast cyclones has been identified (Fig. 14), especially in the past decade. This trend is significant at the 99% level (Table 4). Because of the careful selection of stations and the objective nature of the analysis, this trend does not arise from changing practices. It is readily apparent above the high interannual variability, with the mean for the last decade being nearly twice that for the first decade.

No corresponding significant annual trend for the STAC, HRO, SOI, and interannual differences of the SOI is identified (Table 4). The annual trend for increased numbers of ECC is associated with an increase of ECC in the autumn months, when there appears to be a poleward shift of the STAC from its mean position and an increase in heavy-rain occurrences.

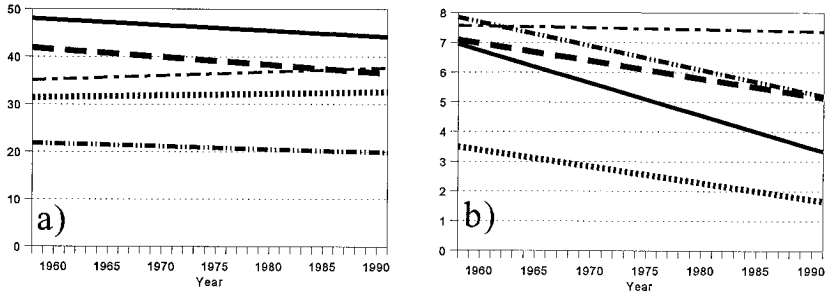

FIG. 13. Summary of linear trends over the period 1958–91, for (a) heavy-rain occurrences and (b) local convective heavy-rain events. Data is averaged into regions of 20°–25°S (–·–); 25°–30°S (– –); 30°–35°S (———;); 35°–37.5°S (··); and 37.5°–40°S (–··–··).

4. Discussion and conclusions

We have examined the incidence of Australian east-coast cyclones and heavy-rain events for the period January 1958 to September 1992. The basis of the analysis is an objective interpretation of rainfall and wind observations from 28 observing stations along the Australian east coast. East coast cyclones are objectively defined by rainfall and surface wind characteristics. Heavy rain is defined as 10 times the monthly mean rainfall at any station and includes both events covering several stations and days and local convective rainfall that is isolated to one station and less than one day.

South to southeasterly onshore flow is most commonly associated with heavy rain on the east coast of Australia. The latitudinal location and movement of the subtropical anticyclone, and variations in the Southern Oscillation index have been found to be major factors in the variability of coastal heavy-rain occurrences. A poleward shift of the STAC from its mean position is associated with heavy-rain occurrences. This synoptic situation is conducive to onshore flow, where topographic or local effects would sustain heavy rainfall. The maximum frequency of heavy-rain occurrences, moves equatorward from summer to winter, mimicking the movement of the STAC. The frequency of local convective heavy-rain events decreases with increasing latitude and no seasonal movement with latitude was detected.

The reasons for strong positive correlation between heavy-rain occurrences and the SOI are not so obvious. Van Loon and Shea (1985) suggested that strong easterlies were associated with La Niña episodes (wet years in Australia), and Pittock (1973) and Lough (1991) demonstrated a poleward shift of the STAC with high SOI in the summer months. Our finding also demonstrates a significant linear correlation between the STAC and SOI, annually and in summer. However, this correlation appears to be highly influenced by the mutual associ-

TABLE 4. Linear correlation coefficients (r), for trends over a defined time period, of local convective heavy-rain events (LCE), HRO, the SOI, interannual differences with the SOI, ECC, and the latitudinal position of the STAC.

Annual linear trend correlations HRO and local convective heavy-rain events (LCE), (1958–91); n = 34

	20°–25°S	25°–30°S	30°–35°S	35°–35.7°S	35.7°–40°S
$r_{hro,yr}$	0.07	−0.144	−0.088	0.026	−0.012
$r_{lce,yr}$	−0.184	−0.252*	−0.401**	−0.288**	−0.4**

Trend correlations, SOI, all HRO, ECC (1958–91)

	Annual n = 33	Seasonal n = 135	Summer n = 33	Autumn n = 34	Winter n = 34	Spring n = 34
$r_{soi,time}$	−0.137	−0.152	−0.149	−0.228*	−0.126	−0.123
$r_{hro,time}$	0.198	0.086	−0.133	0.303**	0.079	0.07
$r_{ecc,time}$	0.379**	0.2	0.133	0.444**	0.139	0.094

Linear trend correlations STAC (1958–81)

	Annual n = 24	Seasonal n = 95	Monthly n = 288	Summer n = 23	Autumn n = 24	Winter n = 24	Spring n = 24
$r_{stac,time}$	0.163	0.073	0.064	0.178	−0.279*	0.382**	0.101

Linear trend correlations of the interannual differences of the SOI (1958–91)

	$SOI_{(yr+1)-yr}$, yr n = 32	$SOI_{(yr+1)-(yr-1)}$, yr n = 31
r	−0.015	0.027

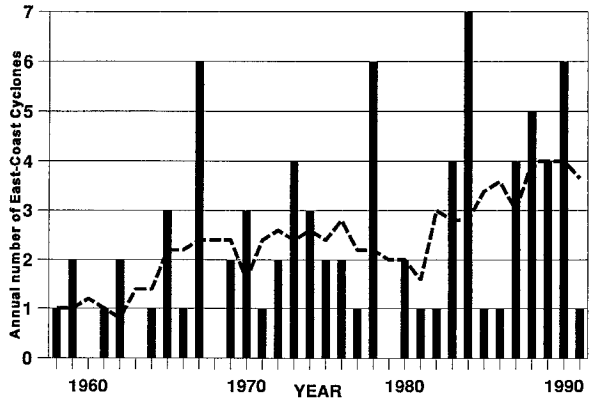

FIG. 14. Time series of the annual occurrence of east coast cyclones (bar graph) together with a 5-yr running average (dashed line).

ation with coastal heavy-rain occurrences. Partial correlations with HRO held constant are significantly lower, which suggests that a poleward shift of the STAC in winter is associated with low SOI. This concurs with Drosdowsky (1988), who also found an increase in easterly trades under the same conditions. Lag correlations show a high (low) frequency of heavy-rain occurrences in spring is associated with a poleward (equatorward) shift of the STAC in the previous summer, autumn, and winter.

Eighty east coast cyclones with 1144 associated heavy-rain occurrences, have been identified for the study period 1958–92. This demonstrates that over 16% of all coastal heavy rainfall between 20° and 40°S is directly related to east coast cyclones. Our dataset of east coast cyclones, in conjunction with figures supplied by the Insurance Council of Australia,[1] suggest that around 7% of all major Australian disasters since 1967 can be directly attributed to east coast cyclones.

Australian east coast cyclones are primarily a cold season, meso-synoptic-scale system. They develop in a synoptic situation conducive to the release of large quantities of latent heat as moist oceanic air is transported westward from a relatively warmer ocean to a cooler continental environment. The resulting forced uplift is enhanced by local topography. East coast cyclones appear to form in regions of warm SST anomalies, due to the position of the East Australian Current or warm core anticyclonic oceanic eddies. However, we found no consistent relationship between intensification of east coast cyclones and warm SST anomalies. Intensification is typically associated with a zonal SST gradient of >4°C within 50 km of the coastline. Below 34°S the East Australian Current becomes a highly dynamical system. The existence of multiple eddies makes correlations with ECC difficult, as one would have to determine the actual path of the cyclone and its relation to local SST or SST gradients. This makes comparisons with the null case, when no east coast cyclones occur, impossible as one would not know which SST anomaly or SST gradient to use. However, we found no consistent relationship between intensification of east coast cyclones and the magnitude of warm SST anomalies.

As expected, from using heavy-rain days in defining east coast cyclones, there is a strong correlation between HRO and ECC. There is considerable interannual variability in the frequency of ECC, with some years producing many ECC and there being none in other years. No direct annual relationship between this variability and the STAC or SOI has been identified. But there is a strong tendency for Australian east coast cyclones to occur after El Niño years and in particular between large swings of negative to positive SOI values. The quasi-biennial cycle associated with ENSO variability (van Loon and Shea 1985; Meehl 1987; Rasmusson et al. 1990) demonstrates a preference for El Niño years to be preceded or followed by La Niña years. This suggests that ECC tend to be more frequent in the transition period between El Niño and La Niña episodes. A possible physical explanation for this may be provided by the preference for tropical cyclones to form closer to the east coast of Australia in La Niña years and farther east in El Niño years (Hastings 1990). We speculate that the large-scale synoptic conditions conducive to the formation of ECC may also shift westward between El Niño and La Niña episodes.

On a seasonal timescale, there is a strong winter correlation between the SOI and ECC, after the effects of HRO have been removed. Increased numbers of ECC are associated with a strong negative SOI, which in turn is related to a poleward shift of the STAC from its mean, and increased heavy-rain occurrences. A poleward shift of the STAC in autumn is associated with a significant increase in ECC and HRO. This may be a consequence of late season tropical cyclones moving into higher latitudes.

No significant long-term trend has been identified for widespread heavy-rain occurrences. However, the number of local convective heavy-rain events has decreased over the last three decades, especially in the higher latitudes.

A major finding is that the numbers of east coast cyclones has nearly doubled in the past 30 yr, and this trend is highly significant. We found no clear evidence that there has been any similar long-term trend in HRO, the SOI, interannual differences of the SOI, or the position of the subtropical anticyclone to justify any concept of large-scale climatic change. However, Zhang and Casey (1992) identify a sustained positive trend of the SOI (defined as a continuing increase in succeeding SOI maxima, separated by about 4 yr) between 1976 and 1989, consistent with our findings of increased numbers of east coast cyclones over the same period. This suggests that the use of SOI phase relationships, such as

[1] Insurance Council of Australia Limited. Major disasters since June 1967. Revised to January 1991.

employed by Stone and Auliciems (1992), may be of benefit in understanding the frequency of east coast cyclones in future work.

The method used to objectively identify cyclones and rain events will tend to underestimate the actual frequency slightly, due to the possibility of two or more systems contributing to one heavy-rain event. This is especially a problem in identifying the small type 1 and 3 events that are associated with larger cyclones. Nevertheless, the method is stable and not subject to vagaries of analysis technique and changing observing systems. Such an approach may be used to identify other heavy rain producing mesoscale systems such as frontal systems and the more intense southerly busters.

Acknowledgments. The authors are grateful to the Sydney Regional Weather Bureau for their support, Maciej Skierski for organizing the rainfall dataset into heavy-rain days, and the three anonymous reviewers for their valuable comments. This study has been partially supported by the U.S. Office of Naval Research under Grant N-0014-89-J1737, and by an APRA Industry Scholarship.

REFERENCES

Allan, R. J., K. Beck, and W. M. Mitchell, 1990: Sea level and rainfall correlations in Australia: Tropical links. *J. Climate,* **3,** 838–846.

Andrews, J. C., 1979: Eddy structure and the West and East Australian Currents. Flinders Institute for Atmospheric and Marine Sciences Res. Rep., 172 pp. [Available from Flinders University of South Australia, Sturt Rd., Bedford Park, South Australia, Australia.]

Callaghan, J., 1986: Subtropical cyclogenesis off Australia's east coast. *Extended Abstracts, Second Int. Conf. on Southern Hemisphere Meteorology,* Wellington, New Zealand, Amer. Meteor. Soc., 38–41.

Cordery, I., and Y. Opoku-Ankomah, 1994: Temporal variation of relations between tropical sea-surface temperatures and New South Wales rainfall. *Aust. Meteor. Mag.,* **43,** 73–80.

Drosdowsky, W., 1988: Lag correlations between the Southern Oscillation and the troposphere over Australia. Bureau of Meteorology Res. Rep. 13, 201 pp. [Available from Bureau of Meterology, GPO Box 1289K, Melbourne, Victoria, Australia.]

Harmon, B. V., 1961: The structure of the East Australian Current. Division of Fisheries and Oceanography Tech. Paper 11, 11 pp. [Available from Commonwealth Scientific and Industrial Research Organisation, 150 Oxford St., Collingwood, Victoria, Australia.]

Hastings, P. A., 1990: Southern Oscillation influences on tropical cyclone activity in the Australian/Southwest Pacific region. *Int. J. Climatol.,* **10,** 291–298.

Holland, G. J., A. H. Lynch, and L. M. Leslie, 1987: Australian east-coast cyclones. Part I: Synoptic overview and case study. *Mon. Wea. Rev.,* **115,** 3024–3036.

Kiladis, G. N., and H. F. Diaz, 1989: Global climatic anomalies associated with extremes in the southern oscillation. *J. Climate,* **2,** 1069–1090.

Lavery, B. M., A. P. Kariko, and N. Nicholls, 1992: A high-quality historical rainfall data set for Australia. *Aust. Meteor. Mag.,* **40,** 33–39.

Leslie, L. M., G. J. Holland, and A.H. Lynch, 1987: Australian east-coast cyclones. Part II: Numerical modeling study. *Mon. Wea. Rev.,* **115,** 3037–3053.

Lough, J. M., 1991: Rainfall variations in Queensland, Australia: 1891–1986. *Int. J. Climatol.,* **11,** 745–768.

——, 1992: Variations of sea-surface temperatures off north-eastern Australia and associations with rainfall in Queensland: 1956–1987. *Int. J. Climatol.,* **12,** 765–782.

Lynch, A. H., 1987: Australian east-coast cyclones. Part 3: Case study of the storm of August 1986. *Aust. Meteor. Mag.,* **35,** 163–170.

McInnes, K. L., and G. D. Hess, 1992: Modifications to the Australian region limited area model and their impact on an east coast low event. *Aust. Meteor. Mag.,* **40,** 21–31.

——, L. M. Leslie, and J. L. McBride, 1992: Numerical simulation of cut-off lows on the Australian east coast: Sensitivity to sea-surface temperature. *Int. J. Climatol.,* **12,** 1–13.

Meehl, G. A., 1987: The annual cycle and interannual variability in the tropical Pacific and Indian Ocean regions. *Mon. Wea. Rev.,* **115,** 27–50.

Moore, D. S., and G. P. McCabe, 1993: *Introduction to the Practice of Statistics*. Freeman, 854 pp.

Nicholls, N., 1984: The Southern Oscillation, sea-surface temperature, and the interannual fluctuations in Australian tropical cyclone activity. *J. Climatol.,* **4,** 661–670.

——, 1985: Predictability of interannual variations of Australian seasonal tropical cyclone activity. *Mon. Wea. Rev.,* **113,** 1144–1149.

——, 1992: Recent performance of a method for forecasting Australian seasonal tropical cyclone activity. *Aust. Meteor. Mag.,* **40,** 105–110.

——, and A. Kariko, 1993: East Australian rainfall events: Interannual variations, trends, and relationships with the Southern Oscillation. *J. Climate,* **6,** 1141–1152.

Pittock, A. B., 1973: Global meridional interactions in stratosphere and troposphere. *Quart. J. Roy. Meteor. Soc.,* **99,** 424–437.

Rasmusson, E. M., X. Wang, and C. F. Ropelewski, 1990: The biennial component of ENSO variability. *J. Mar. Sci.,* **1,** 71–96.

Ropelewski, C. F., and M. S. Halpert, 1987: Global and regional scale precipitation patterns associated with the El Niño/Southern Oscillation. *Mon. Wea. Rev.,* **115,** 1606–1626.

——, and ——, 1989: Precipitation patterns associated with the high index phase of the Southern Oscillation. *J. Climate,* **2,** 268–284.

Sanders, F., and J. R. Gyakum, 1980: Synoptic-dynamic climatology of the ''bomb.'' *Mon. Wea. Rev.,* **108,** 1589–1606.

Sinclair, M. R., 1994: An objective cyclone climatology for the Southern Hemisphere. *Mon. Wea. Rev.,* **122,** 2239–2256.

Speer, M., and B. Geerts, 1994: A synoptic-mesoalpha-scale climatology of flash-floods in the Sydney metropolitan area. *Aust. Meteor. Mag.,* **43,** 87–103.

Stone, R., and A. Auliciems, 1992: SOI phase relationships with rainfall in eastern Australia. *Int. J. Climatol.,* **12,** 625–636.

Streten, N. A., 1983: Extreme distributions of Australian annual rainfall in relation to sea-surface temperature. *J. Climatol.,* **3,** 143–153.

van Loon, H., and D. J. Shea, 1985: The Southern Oscillation. Part IV: The development of warm and cold events. *Mon. Wea. Rev.,* **113,** 2063–2074.

Whetton, P., D. Adamson, and M. Williams, 1990; Rainfall and river flow variability in Africa, Australia, and East Asia linked to El Niño–Southern Oscillation events. *Geol. Soc. Aust. Symp. Proc.,* **1,** 71–82.

Yu, B., and D. T. Neil, 1991: Global warming and regional rainfall: The difference between average and high intensity rainfalls. *Int. J. Climatol.,* **11,** 653–661.

Zhang X.-G., and T. M. Casey, 1992: Long term variations in the Southern Oscillation and relationships with Australian rainfall. *Aust. Meteor. Mag.,* **40,** 211–225.

APPENDIX
Detailed Information for the 28 Coastal Stations Used in the Study.
All stations are still in operation except where otherwise stated.

Station	Name	Latitude Longitude	Elevation meters	Operational dates
1	Hayman Island	−20°03′ −148°53′	2.0	1934–
2	Mackay Met. Office	−21°07′ −149°13′	6.0	1959–
3	Mackay Airport	−21°10′ −149°11′	6.0	1950–59
4	St. Lawrence	−22°21′ −149°32′	11.0	1870–
5	Gladstone	−23°51′ −151°16′	76.0	1957–
6	Bundaberg Post Office	−24°52′ −152°21′	31.0	1942–
7	Bundaberg Airport	−24°54′ −152°19′	14.0	1957–
8	Maryborough	−25°33′ −152°41′	11.0	1883–
9	Tewantin	−26°24′ −153°02′	8.0	1895–
10	Brisbane Met. Office	−27°23′ −153°07′	4.0	1929–
11	Cape Byron	−28°38′ −153°38′	91.0	1948–
12	Yamba	−29°26′ −153°22′	29.0	1877–
13	Coffs Harbour	−30°19′ −153°07′	5.0	1943–
14	Smoky Cape	−30°55′ −153°05′	117.0	1939–
15	Port Macquarie	−31°27′ −152°55′	7.0	1840–
16	Williamtown	−32°48′ −151°50′	9.0	1942–
17	Newcastle	−32°55′ −151°48′	33.0	1862–
18	Nora Head	−33°17′ −151°35′	27.0	1969–
19	Sydney Airport	−33°56′ −151°10′	6.0	1929–
20	Nowra	−34°57′ −150°32′	109.0	1942–
21	Moruya Heads	−35°55′ −150°09′	17.0	1875–
22	Merimbula Airport	−36°55′ −149°54′	2.0	1961–
23	Green Cape	−37°16′ −150°03′	18.0	1904–
24	Gabo Island	−37°34′ −149°55′	15.0	1959–
25	Sale East	−38°06′ −147°09′	5.0	1943–
26	Wilsons Promontory	−39°08′ −146°25′	89.0	1872–
27	King Island	−39°56′ −143°51′	24.0	1909–
28	Flinders Island	−40°06′ −148°00′	7.0	1942–